

# Synthesis of PGE sulfide standards for laser ablation inductively coupled plasma mass spectrometry (LA-ICP-MS)

Cora C. Wohlgemuth-Ueberwasser · Chris Ballhaus ·  
Jasper Berndt · Vaida Stotter née Paliulionyte ·  
Thomas Meisel

Received: 26 January 2007 / Accepted: 30 April 2007 / Published online: 16 June 2007  
© Springer-Verlag 2007

**Abstract** Sulfide compositions with known Re, Os, Ir, Ru, Rh, Pt, and Pd contents are synthesized to be used as standards for noble metal analysis in solid solution in sulfides. Major elements were added as metals and elemental S. The noble metals, i.e. 35 and 60 ppm each, were added as solutions by micro syringe. Following synthesis at 1 atm the sulfides were sintered at 1.5 to 2 GPa to obtain pellets with theoretical density. Aliquots of the pellets were analysed by isotope dilution ICP-MS for bulk Re and platinum-group elements (PGE). The spatial noble metal distribution was investigated with an ArF excimer laser coupled to a single collector ICP mass spectrometer. Sample homogeneity is shown to depend on the metal/S spectrum and the major element composition of the sulfide, as well as on more subtle factors like oxygen partial pressure during synthesis, run temperature, and degree of partial melting. The most homogeneous sulfide composition is a  $(\text{Fe,Ni})_{1-x}\text{S}$  monosulfide with 5 wt % Ni and 1-sigma variations in  $^{34}\text{S}$ -normalized noble metal count rates of <3.6%. Nearly as homogeneous is a pure  $\text{Fe}_{1-x}\text{S}$  monosulfide with 1-sigma variations in  $^{34}\text{S}$ -normalized noble metal count rates of <5.8 %. A Cu-bearing  $\text{Fe}_{1-x}\text{S}$

monosulfide with 2 wt % Cu was found to be considerably more heterogeneous, suggesting that Cu in solid solution in monosulfides promotes noble metal heterogeneity. The sulfide composition least suitable for the synthesis of noble metal sulfide standards is NiS.

**Keywords** Laser-ablation-ICP-MS · Platinum-group elements · Sulfide standard material · Pyrrhotite · Piston cylinder

## Introduction

The highly siderophile elements Re, Os, Ir, Ru, Rh, Pt, and Pd (HSE) not only are economically valuable elements, they also serve as geochemical tracers to understand magma genesis in the upper mantle, mantle evolution, and core-mantle equilibria during early Earth differentiation (e.g. Bockrath et al. 2004a). In natural rocks, the HSE occur to a large extent in solid solution in base metal sulfides, notably in pyrrhotite and pentlandite. In sulfide-poor lithologies and in rocks unusually rich in platinum-group elements (PGE), we also find discrete PGE sulfides and alloys, PGE arsenides, and intermetallic compounds of the PGE with Sb, Te, and Bi (Ballhaus and Stumpfl 1986; Gervilla et al. 2002; Bockrath et al. 2004b; Miller et al. 2005; Helmy et al. 2007).

HSE concentrations in base metal sulfides typically are in the low ppm to high ppb concentration range. Usually, in-situ concentrations in sulfides are quantified with laser-ablation inductively coupled mass spectrometry (LA-ICP-MS; Huminicki et al. 2005). Compared with other in-situ analytical techniques such as SIMS or PIXE (Ballhaus and Ryan 1995; Cabri et al. 2003), LA-ICP-MS offers a number of advantages, including cost efficiency, detection limits in

---

Communicated by Jochen Hoefs.

---

C. C. Wohlgemuth-Ueberwasser (✉) · J. Berndt  
Institut für Mineralogie, Universität Münster,  
Corrensstr. 24, 48149 Münster, Germany  
e-mail: ueberwas@uni-muenster.de

C. C. Wohlgemuth-Ueberwasser · C. Ballhaus  
Mineralogisches Institut und Museum, Universität Bonn,  
Poppelsdorfer Schloss, 53115 Bonn, Germany

V. Stotter née Paliulionyte · T. Meisel  
General and Analytical Chemistry, University of Leoben,  
Franz-Josef-Str. 18, 8700 Leoben, Austria

the low ppb range under optimum conditions, the ability to monitor 3D trace element distributions, and the capability to discriminate between HSE in solid solution and HSE in discrete micronuggets (e.g. Ballhaus and Sylvester 2000). Disadvantages are the large spot sizes of  $>25\ \mu\text{m}$  to ablate a sufficient amount of material which require a minimum grain size for a reliable analysis of 40 to 50  $\mu\text{m}$ , plus the fact that LA-ICP-MS is destructive. Hence, individual analyses are not reproducible and the life time of standards used for laser-ablation analysis is limited.

For this reason, most LA-ICP-MS laboratories now synthesize their own standards for sulfide analysis. A commonly used synthesis method is by nickel sulfide fire assay (Date et al. 1987; Jackson et al. 1990; Jarvis et al. 1995; Chenery et al. 1995; Shibuya et al. 1998). In this technique, a PGE-bearing rock is equilibrated with NiS and a sodium carbonate/sodium tetraborate flux at superliquidus temperature. A sulfide melt is segregated, and the chalcophile and siderophile elements of the rock sample are sequestered to the sulfide. After bulk noble metal analysis, aliquots of the Ni sulfide button are used for laser ablation analysis. Unfortunately, neither the major element nor the trace element abundances in the sulfide can be controlled well during sulfide collection, and the phase relations of the quenched sulfide are also unpredictable. Alard and Horn (pers. comm. 2006) report that their Ni sulfide fire assay buttons crystallized two sulfides with differing metal/S atomic ratios which we confirm here, and this can lead to small-scale noble metal fractionations between the phases and impose a chemical heterogeneity on the standard, as shown below. Another disadvantage is that the high Ni content may cause isobaric interferences of  $^{61}\text{Ni}^{40}\text{Ar}$  on  $^{101}\text{Ru}$ . This may complicate Ru analysis in Pd-bearing samples where  $^{102}\text{Ru}$  cannot be quantified because of interference with  $^{102}\text{Pd}$ .

Ballhaus and Sylvester (2000) synthesized sulfide standards by adding chloride solutions with 5 to 10 ppm Ir, Ru, Rh, Pt, and Pd to synthetic  $\text{Fe}_{1-x}\text{S}$ . After drying the sulfides were equilibrated in  $\text{SiO}_2$  glass capsules in a piston cylinder press at 900°C and 2 GPa to obtain one-phase  $\text{Fe}_{1-x}\text{S}$  monosulfide aggregates with theoretical density. Bulk compositions were analyzed with ICP quadrupole mass spectrometry, and the spatial PGE distribution was tested by checking  $^{34}\text{S}$ -normalized PGE count rate variations with LA-ICP-MS. These standards were widely used for analysis of magmatic sulfides (Ballhaus and Sylvester 2000; Cabri et al. 2003) and for cross-calibration of subsequently synthesized sulfide standard compositions (e.g. Cabri et al. 2003; Mungall et al. 2005) but are now consumed.

Cabri et al. (2003) and Mungall et al. (2005) synthesized sulfide standards at one atm in  $\text{SiO}_2$  glass capsules, using metallic Fe and elemental S mixtures doped with metallic

Ru, Rh, and Pd. After melting at 1205°C, absolute PGE concentrations were determined by cross-calibrating against the Ballhaus–Sylvester standards. Two more 1-atm FeS standards were produced by Sylvester et al. (2005) and Barnes et al. (2006), both with 30 ppm of each PGE and Au. In both studies, emphasis was placed on thorough homogenization, and therefore the synthesis procedure (at 1 atm in  $\text{SiO}_2$  glass) was interrupted by several episodes of regrinding and mechanical homogenization. Noble metal concentrations were subsequently analyzed by solution ICP mass spectrometry (Sylvester et al. 2005) and by isotope dilution mass spectrometry (Barnes et al. 2006). Spatial homogeneity was tested with LA-ICP-MS.

A third method of standard preparation is by cold pressing. Wilson et al. (2002) precipitated amorphous Fe–Cu–Zn sulfides by reducing metal-bearing multi-element sulfate solutions, then pressed the sulfide precipitates to pellets to be used as laser standards. One of these standards (USGS-Standard MASS-1) is reported to contain 50 ppm each of Ir, Pt, and Au (Sylvester et al. 2005), in addition to Ag, As, Bi, Cd, Co, Cr, Ga, Ge, In, Mn, Mo, Sb, Se, and V. The only precious metal well analyzed to date appears to be Au but was later demonstrated with LA-ICP-MS to be distributed heterogeneously (Wilson et al. 2002; Yang et al. 2006; Lehner et al. 2006; Mungall et al. 2005). Perkins et al. (1997) doped sulfide (sphalerite, galena, pyrite, and marcasite) powders with multi-element (Ni, Zn, As, Se, Mo, Ru, Rh, Pd, Ag, Te, Au and Bi) solutions and pressed the powders to pellets using vinyl alcohol as a binder. Homogeneity was tested with LA-ICP-MS and reported to be between 5 and 10 relative percent. We do not have experience with pressed powder standards but suspect that they may have ablation characteristics different to sulfides synthesized at high temperature.

This paper outlines the synthesis conditions most suitable for the preparation of homogeneous sulfide standards for in-situ noble metal analysis. The study is motivated by the fact that LA-ICP-MS analysis is destructive and that standards are consumables. Hence, analysts are often forced to produce their own sulfide standard compositions with specific trace element spectra, depending on the compositions of the unknowns. The compositions reported here are  $(\text{Fe,Ni,Cu})_{1-x}\text{S}$  monosulfides synthesized from metals and elemental S. Re and PGE concentrations range from 35 to 60 ppm per metal. We show that sulfide homogeneity not only depends on the degree of mechanical homogenization of the starting mixes and the sulfide products (cf. Sylvester et al. 2005) but also on subtle factors like capsule material, synthesis temperature, oxygen partial pressures during sulfide synthesis, and major element composition of the sulfide matrix. For the first time, we report how variations in laser beam diameter, laser beam energy, and major element sulfide composition will

affect the precision of noble metal analysis in sulfides. Our most homogeneous sulfide compositions have variations in Re and PGE concentrations of less than four relative percent.

### Synthesis of sulfide starting materials

The starting sulfide compositions were  $\text{Fe}_{0.9}\text{S}$ , a  $(\text{Fe,Ni})_{1-x}\text{S}$  monosulfide solid solution with 5 wt % Ni, a  $(\text{Fe,Cu})_{1-x}\text{S}$  monosulfide with 2 wt % Cu, and a pure  $\text{Ni}_{0.95}\text{S}$  sulfide. All compositions were kept on the metal-deficient side in order to enhance PGE solubility. Ballhaus and Ulmer (1995) and Li et al. (1996) observed that the solubility of PGE in  $\text{Fe}_{1-x}\text{S}$ -rich monosulfides increases with decreasing metal/S atomic ratio, notably the solubilities of Pt and Pd.

All compositions were synthesized from Fe, Ni, Cu metal powders and elemental sulfur, following the procedure of Ballhaus et al. (2006). The PGE were added as chloride solutions and Re as a nitrate solution. To prevent oxidation of the metals during addition of the PGE-bearing acids, in particular of metallic Fe, the noble metal solutions were added to the elemental sulfur fractions of each mix. The sulfur powder was then dried at 60°C for several hours until complete acid evaporation, and only then were the base metal powders Fe, Ni, and Cu added and homogenized with S.

After thorough homogenization in an agate mortar, the starting mixes were sealed under vacuum in  $\text{SiO}_2$  glass tubes. Prior to welding, the tubes and the sample powders were repeatedly evacuated and flushed with Ar, to replace all trapped air and prevent formation of undesired phases like magnetite. Each sulfide composition was then reacted stepwise at 200, 300, 500 and 900°C over about 30 h, to obtain homogeneous, single-phase monosulfide crystals. Since the reaction of metal powder with elemental S to sulfide is highly exothermic, temperature should initially be raised very carefully in small steps until all elemental S, evident as brownish precipitates along the capsule walls, is consumed. At no stage during sulfide synthesis should temperatures rise above the solidus temperature of the sulfide, in order to prevent partial melting.

Synthesis at 1 atm produces coarsely crystalline, loose aggregates of hexagonal monosulfide crystals. These were then ground for about 30 min in an agate mortar to grain sizes around 10  $\mu\text{m}$ . Subsequently, ~ 250 mg of each sulfide powder were reacted in a piston cylinder press at high temperature (900–1200°C) and pressure (1.5–2 GPa) to produce homogeneous, single-phase monosulfide aggregates with theoretical density. Compositional heterogeneities that might have survived the 1-atm synthesis steps can possibly be ironed out at this stage by intracrystalline dif-

fusion of noble metals in the sulfide lattice. Our experience is that the sintering temperature should be as high as possible but should remain below the solidus temperature of the sulfide composition, because partial melting may impose PGE heterogeneity by causing the metals to fractionate between crystalline monosulfide and sulfide melt. The pure  $\text{Fe}_{1-x}\text{S}$  and the Ni-bearing  $(\text{Fe,Ni})_{1-x}\text{S}$  monosulfides were sintered at 1100°C and the Cu-bearing  $(\text{Fe,Cu})_{1-x}\text{S}$  composition at 900°C. These temperatures are at least 50°C below the respective solidus temperatures. From the pure NiS composition, we prepared two charges, one at 880°C and another at 1200°C. Later BSE imaging showed that the 1200°C charge was well above the solidus temperature of NiS.

It was surprising to note how strongly the capsule material influences noble metal distribution in the sulfides. We have employed several capsule materials in common use in high-pressure experimentation, including boron nitride (BN), graphite, and MgO. Theoretically, all these materials should be inert toward sulfide, however, in practice all three imposed small-scale PGE heterogeneity. For example, sulfides sintered in BN showed noble metal heterogeneities of the order of 60% in  $^{34}\text{S}$ -normalized count rate variations. Very often, individual laser spectra showed PGE spikes that we attribute to discrete PGE phases (cf. Ballhaus and Sylvester 2000). The same was observed with sulfides equilibrated in graphite and in MgO capsules. How and why these materials cause PGE heterogeneity is not well understood, but evidently they lower noble metal solubilities to a degree that discrete PGE phases may precipitate.

Therefore, all subsequent sulfide sinterings were carried out in  $\text{SiO}_2$  glass capsules. The capsules were prepared from 6/4 mm outer/inner diameter  $\text{SiO}_2$  tubes, welded shut on one side and sealed on the other by a 1 mm long borosilicate glass plug. Borosilicate glass becomes plastic at about 550°C and seals the capsule reliably against atmosphere already during the heating phase of an experiment, avoiding possible sulfide oxidation. So long as no partial sulfide melt is present, the danger of capsule leakage and sulfide loss is small.

After sintering, about one third of each charge was polished for microprobe and laser-ablation analysis. The remainder was kept for later Re and PGE bulk analysis by isotope dilution (ID) ICP-MS.

### Analytical conditions

The major elements Fe, Ni, Cu, and S were analysed by electron microprobe (EMP) using natural sulfides as standards (cf. Table 1). Re and PGE distributions were tested by LA-ICP-MS using an 193 nm ArF excimer laser cou-

**Table 1** Major element compositions (in wt %) of monosulfide phases of the four starting sulfide compositions  $(\text{Fe,Ni})_{1-x}\text{S}$ ,  $(\text{Fe,Cu})_{1-x}\text{S}$ ,  $\text{Fe}_{1-x}\text{S}$ , and  $\text{Ni}_{1-x}\text{S}$ , as determined by electronmicroprobe. The NiS composition quenches out two sulfide phases with different metal/S atomic ratios (see text). Averages of  $n$  analyses per phase with 1-sigma standard deviations

	$(\text{Fe,Ni})_{1-x}\text{S}$ ( $n = 20$ )	$(\text{Fe,Cu})_{1-x}\text{S}$ ( $n = 20$ )	$\text{Fe}_{1-x}\text{S}$ ( $n = 19$ )	NiS ( $n = 10$ )	$\text{Ni}_{6-x}\text{S}_5$ ( $n = 10$ )
Fe	$55.4 \pm 0.20$	$58.2 \pm 0.16$	$60.5 \pm 0.25$	$0.01 \pm 0.01$	$0.01 \pm 0.01$
Ni	$4.72 \pm 0.04$	$0.01 \pm 0.01$	$0.01 \pm 0.01$	$63.6 \pm 0.40$	$66.9 \pm 0.49$
Cu	$0.01 \pm 0.01$	$2.15 \pm 0.04$	$0.01 \pm 0.01$	$0.01 \pm 0.01$	$0.01 \pm 0.01$
S	$39.1 \pm 0.29$	$38.3 \pm 0.23$	$39.1 \pm 0.23$	$35.1 \pm 0.38$	$31.4 \pm 0.49$
Metal/S (at%)	$0.88 \pm 0.01$	$0.88 \pm 0.01$	$0.88 \pm 0.01$	$0.99 \pm 0.02$	$1.16 \pm 0.04$

pled to single collector magnetic sector ICP mass spectrometer (Finnigan Thermo Element 2). The carrier gas into which ablation took place was He. Compared to Ar, He minimizes sample redeposition out of the aerosol and stabilizes signal intensities (Eggins et al. 1998; Günther and Heinrich 1999; Horn et al. 2001). Each standard was analysed with about 20 laser spots, randomly distributed across the charge.

A typical laser ablation spectrum reduced to some elements is shown in Fig. 1. Isotopes recorded were  $^{34}\text{S}$ ,  $^{60}\text{Ni}$ ,  $^{63}\text{Cu}$ ,  $^{99}\text{Ru}$ ,  $^{101}\text{Ru}$ ,  $^{102}\text{Ru}$ ,  $^{103}\text{Rh}$ ,  $^{105}\text{Pd}$ ,  $^{106}\text{Pd}$ ,  $^{108}\text{Pd}$ ,  $^{185}\text{Re}$ ,  $^{187}\text{Re}$ ,  $^{189}\text{Os}$ ,  $^{190}\text{Os}$ ,  $^{192}\text{Os}$ ,  $^{191}\text{Ir}$ ,  $^{193}\text{Ir}$ ,  $^{194}\text{Pt}$ , and  $^{195}\text{Pt}$ . One sweep for these masses took about 1 s within which each isotope was counted four times. Each spectrum consisted of 60 to 80 sweeps on the sample, preceded by  $\sim 40$  sweeps on the gas background. The first 10 to 20 s of a laser spectrum, in Fig. 1 from 56 to 74 s, were discarded. Interferences with argides may affect the isotopes  $^{101}\text{Ru}$  ( $^{61}\text{Ni}^{40}\text{Ar}$ ),  $^{103}\text{Rh}$  ( $^{63}\text{Cu}^{40}\text{Ar}$ ), and  $^{105}\text{Pd}$  ( $^{65}\text{Cu}^{40}\text{Ar}$ ), but are so minor that they can be ignored. We verified this by ablating pure Ni and Cu metal for apparent  $^{101}\text{Ru}$ ,  $^{103}\text{Rh}$ , and  $^{105}\text{Pd}$  concentrations with the same conditions as the sulfides. Apparent  $^{101}\text{Ru}$  count rates on metallic Ni, hence assignable to  $^{61}\text{Ni}^{40}\text{Ar}$ , were 197 cps or  $<0.001\%$  of the Ni sig-

nal,  $^{105}\text{Pd}$  count rates on metallic Cu assignable to  $^{65}\text{Cu}^{40}\text{Ar}$  were 725 cps or  $<0.001\%$  of the Cu signal, and apparent  $^{103}\text{Rh}$  count rates ( $^{63}\text{Cu}^{40}\text{Ar}$ ) were 1380 cps or  $0.002\%$  of the Cu count rates. Thus, for a sulfide with 5 and 67% Ni (Table 1), the argide contributions to  $^{101}\text{Ru}$  are  $<1$  and  $\sim 7$  cps. For a sulfide with 2% Cu, the contributions from Cu argides to  $^{105}\text{Pd}$  and  $^{103}\text{Rh}$  are  $\sim 15$  and 28 cps, respectively. These count rates are well within gas background.

All count rates were normalized to  $^{34}\text{S}$  and the average S content of each sulfide as determined by microprobe (Table 1), then averaged over a laser ablation spectrum. By normalizing to  $^{34}\text{S}$ , time-dependent drifts in count rates, evident in the negative slopes of the laser spectra (Fig. 1), are largely eliminated.

#### Noble metal distribution

In Fig. 2, we show the  $^{34}\text{S}$ -normalized count rates of the isotopes  $^{101}\text{Ru}$  and  $^{195}\text{Pt}$ , representative for all other noble metal isotopes. The figure allows assessing sulfide homogeneity. Our most homogeneous sulfides are the  $\text{Fe}_{1-x}\text{S}$  and  $(\text{Fe,Ni})_{1-x}\text{S}$  compositions followed by the  $(\text{Fe,Cu})_{1-x}\text{S}$  composition. The NiS composition is very heterogeneous. The error bars on each average reflect fluctuations in the Ar plasma and changes in the amount of material sequestered to the plasma, i.e. scattering in absolute count rates in Fig. 1, and are thus instrument-related.

Sample homogeneity can also be expressed numerically as the deviation of each average from the mean of all ablation spectra, calculated as one sigma relative standard deviation (RSD) in percent. Note that these RSD do not include the errors displayed in Fig. 2, since these errors are thought to be related mostly to plasma and variations in aerosol supply to the plasma. Results under optimum conditions for each investigated sulfide are as follows: The  $\text{Fe}_{1-x}\text{S}$  composition, sintered at  $1100^\circ\text{C}$  and 2 GPa and analyzed with a laser energy of  $7 \text{ J cm}^{-2}$  and a  $60 \mu\text{m}$  spot size, shows one sigma RSD of 3.5% for  $^{101}\text{Ru}$ , 2.2% for  $^{103}\text{Rh}$ , 2.3% for  $^{105}\text{Pd}$ , 2.7% for  $^{185}\text{Re}$ , 4.1% for  $^{189}\text{Os}$ , 5.1% for  $^{193}\text{Ir}$ , and 3.5% for  $^{195}\text{Pt}$ . This sulfide composition

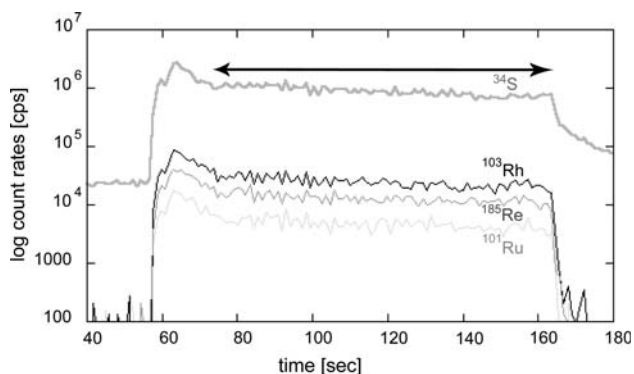
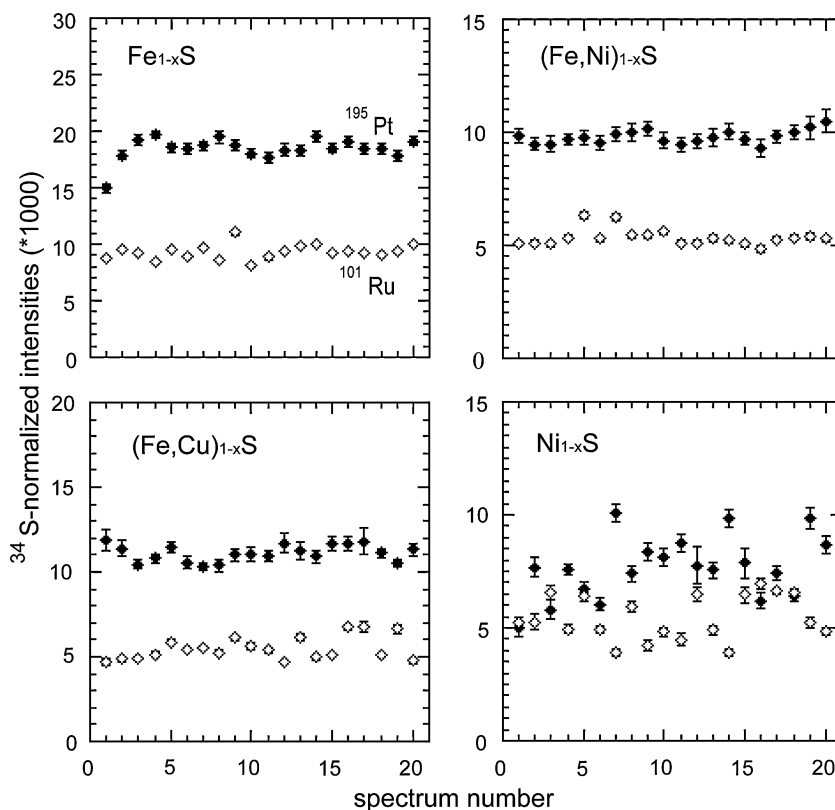


**Fig. 1** Laser ablation spectrum of the  $(\text{Fe,Ni})_{1-x}\text{S}$  sulfide composition showing  $^{34}\text{S}$  and three representative noble metal isotopes. Portion of the spectrum quantified marked by horizontal arrow. Diameter of the laser beam  $60 \mu\text{m}$ , laser energy  $11 \text{ J cm}^{-2}$ , laser frequency 8 Hz

**Fig. 2**  $^{34}\text{S}$ -normalized count rates ( $\times 1000$ ) of the isotopes  $^{101}\text{Ru}$  and  $^{195}\text{Pt}$ , of 20 ablation spectra taken from the  $\text{Fe}_{1-x}\text{S}$ ,  $(\text{Fe,Ni})_{1-x}\text{S}$ ,  $(\text{Fe,Cu})_{1-x}\text{S}$ , and  $\text{Ni}_{1-x}\text{S}$  sulfide compositions (a–d). Error bars are 2 sigma variations about the weighted means and reflect the scatter in the laser spectra evident in Fig. 1. All spectra taken with a  $60\ \mu\text{m}$ ,  $11\ \text{J cm}^{-2}$  laser beam at 8 Hz



crystallized minute amounts of magnetite in addition to monosulfides, mostly concentrated along monosulfide grain boundaries, but we found no evidence that magnetite influences PGE homogeneity or adversely affects sample ablation. We attempted to avoid magnetite by adding traces of boron nitride to the metal-sulfur mixtures to capture oxygen, but as noted above in relation to capsule materials this led to greatly enhanced small-scale Re-PGE heterogeneity.

The Ni-bearing  $\text{Fe}_{1-x}\text{S}$  sulfide composition, sintered at  $1100^\circ\text{C}$  and 2 GPa and analyzed with  $11\ \text{J cm}^{-2}$  and  $60\ \mu\text{m}$ , shows one-sigma RSD of 2.9% for  $^{101}\text{Ru}$ , 2.7% for  $^{103}\text{Rh}$ , 2.6% for  $^{105}\text{Pd}$ , 2.2% for  $^{185}\text{Re}$ , 3.6% for  $^{189}\text{Os}$ , 2.7% for  $^{193}\text{Ir}$  and 3.0% for  $^{195}\text{Pt}$ . Compared with previous standards (Date et al. 1987; Jackson et al. 1990; Jarvis et al. 1995; Chenery et al. 1995; Shibuya et al. 1998; Jorge et al. 1998; Alard et al. 2000; Wilson et al. 2002; Cabri et al. 2003; McDonald 2005; Sylvester et al. 2005), our  $\text{Fe}_{1-x}\text{S}$  and  $(\text{Fe,Ni})_{1-x}\text{S}$  sulfide compositions are among the most homogeneous compositions synthesized to date.

In contrast, the Cu-bearing sulfide composition shows larger variations. With a  $60\ \mu\text{m}$  spot and a laser energy of  $5\ \text{J cm}^{-2}$ , 14 consecutive ablations yielded one-sigma RSD of 9.5% for  $^{101}\text{Ru}$ , 6.8% for  $^{103}\text{Rh}$ , 5.1% for  $^{105}\text{Pd}$ , 8.1% for  $^{185}\text{Re}$ , 9.9% for  $^{189}\text{Os}$ , 7.3% for  $^{193}\text{Ir}$ , and 4.8% for  $^{195}\text{Pt}$ , i.e. variations about twice as large as in the Ni-bearing monosulfide. It seems that Cu, unlike Ni, tends to enhance PGE heterogeneity in FeS-rich monosulfides.

Among the major elements (Table 1), Cu also is the least homogeneously distributed metal in monosulfides.

The pure NiS composition returned the most disappointing results. A charge sintered at  $880^\circ\text{C}$  and 1.5 GPa yielded one-sigma RSD (16 spectra) of 17% for  $^{101}\text{Ru}$ , 13% for  $^{103}\text{Rh}$ , 68% for  $^{105}\text{Pd}$ , 13% for  $^{185}\text{Re}$ , 13% for  $^{189}\text{Os}$ , 12% for  $^{193}\text{Ir}$ , and 60% for  $^{195}\text{Pt}$ . Another charge of that same bulk composition, equilibrated at  $1200^\circ\text{C}$  and 2 GPa at superliquidus conditions, was slightly more homogeneous. With a  $60\ \mu\text{m}$  spot and  $5\ \text{J cm}^{-2}$  laser energy, one-sigma RSD were 17% for  $^{101}\text{Ru}$  and  $^{103}\text{Rh}$ , 13% for  $^{185}\text{Re}$ , 18% for  $^{189}\text{Os}$ , 17% for  $^{193}\text{Ir}$ , and 20% for  $^{105}\text{Pd}$  and  $^{195}\text{Pt}$ . With higher laser energy ( $13\ \text{J cm}^{-2}$ ) RSD decrease but the degree of homogeneity of the  $\text{Fe}_{1-x}\text{S}$  sulfide, and especially the  $(\text{Fe,Ni})_{1-x}\text{S}$  monosulfide composition, is not nearly reached. NiS seems to be an unsuitable matrix for a sulfide-PGE standard. Later examination by BSE imaging revealed that the charge was completely molten and that it quenched out two nickel sulfide phases (Fig. 3), a stoichiometric NiS and a non-stoichiometric  $\text{Ni}_{6-x}\text{S}_5$  compound with  $x < 0.1$ .

#### Optimum conditions for noble metal analysis in sulfide matrix

Having established the degree of homogeneity of each sulfide composition, we then optimized the conditions to

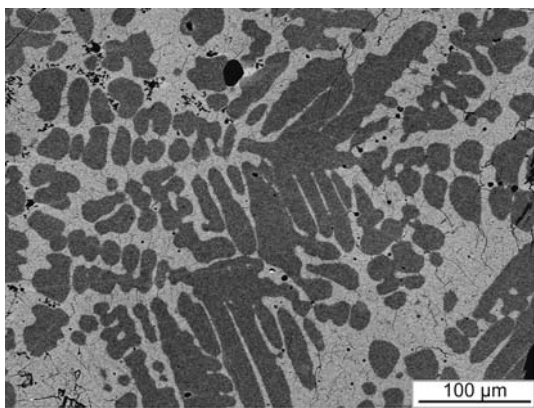


**Fig. 3** Backscattered electron image of the  $\text{Ni}_{1-x}\text{S}$  composition melted at  $1200^\circ\text{C}$  and 2 GPa. Two NiS quench phases with different metal/S ratios in dendritic intergrowth, a near-stoichiometric NiS (dark) and a slightly S-deficient  $\text{Ni}_{6-x}\text{S}_5$  phase (bright)

analyse Re and the PGE in sulfide matrix. Parameters tested include diameter of the laser beam or spot size and the laser energy. The spot size, in  $\mu\text{m}$ , determines the amount of ablated material. Spot size variations allow to determine the scale at which chemical PGE heterogeneities (if any) occur. The laser energy, in  $\text{J cm}^{-2}$ , influences both the amount of material ablated and the temperature at the ablation site. Depending on the thermal conductivity of the target material, it determines whether or not the laser beam will trigger melting. The laser frequency, another parameter of potential significance, was not varied but set to 8 Hz.

Typical ablation craters produced are shown in Fig. 4. With an energy of  $3 \text{ J cm}^{-2}$ , the laser produces well-defined craters with sharp rims, near-constant depths, and

clean crater peripheries (Fig. 4a). Judging from the BSE image, the energy distribution across the beam must be near-uniform. At this low energy, deposits of ablated material at the crater rim are minimal but inside the crater we note a network of elongate crystallites with smooth surfaces, reminiscent of a film of sulfide melt rapidly quenched after the laser was turned off. Higher energies produce more strongly frayed crater rims and more significant degrees of melting, evident by sulfide melt droplets ejected from the crater and deposited around crater peripheries (Fig. 4b and c). Figure 4 c and d show two craters produced with the same energy but on different sulfide compositions. These images reveal that partial melting not only depends on the laser energy but also on the melting point of the sulfide, in that the  $(\text{Fe,Cu})_{1-x}\text{S}$  composition with the lower melting point shows more extensive melting than the refractory  $(\text{Fe,Ni})_{1-x}\text{S}$  composition.

Laser energy also influences the  $^{34}\text{S}$  normalized count rate ratios. In Fig. 5, we show count rates ratios for three representative isotopes ( $^{101}\text{Ru}$ ,  $^{103}\text{Rh}$ ,  $^{195}\text{Pt}$ ), measured on the most homogeneous  $(\text{Fe,Ni})_{1-x}\text{S}$  and the more heterogeneous  $(\text{Fe,Cu})_{1-x}\text{S}$  compositions. Each data point in the diagram is the average of 15 to 20 consecutive ablations. The isotopes were selected according to their partitioning behaviour between monosulfide and sulfide melt; Ru as an element highly compatible with monosulfide, Rh as a moderately compatible element, and Pt as an element highly incompatible with monosulfide. Thus, if during ablation partial melting occurs in the sulfide target, these elements would be expected to fractionate according to their monosulfide–sulfide melt partition coefficients.

**Fig. 4** BSE images of ablation craters produced with variable laser energies. a–c 3, 9, and  $13 \text{ J cm}^{-2}$  on the  $(\text{Fe,Cu})_{1-x}\text{S}$  composition, and d  $13 \text{ J cm}^{-2}$  on the  $(\text{Fe,Ni})_{1-x}\text{S}$  composition. Degree of partial melting (see text) increases with laser energy and melting point of the sulfide. All craters produced with 20 shots and laser beam diameters of  $60 \mu\text{m}$

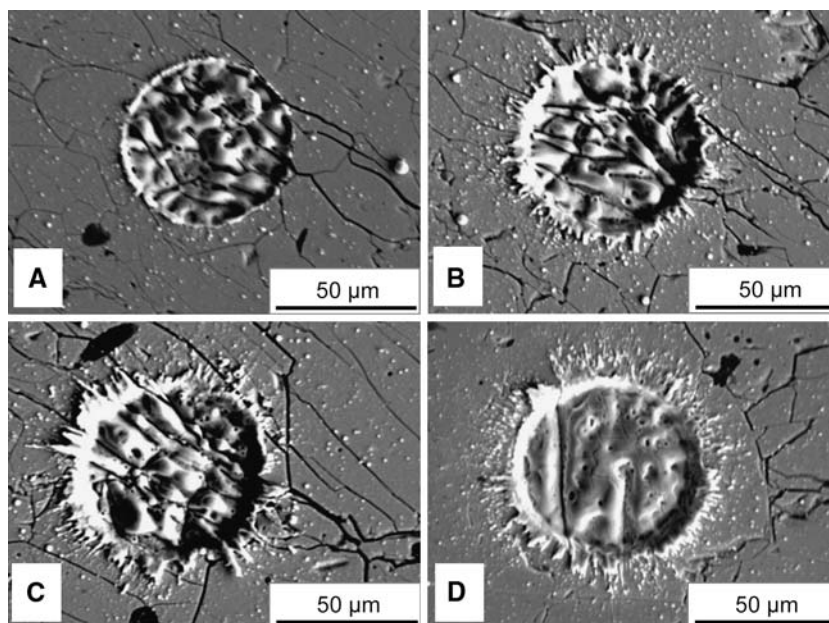
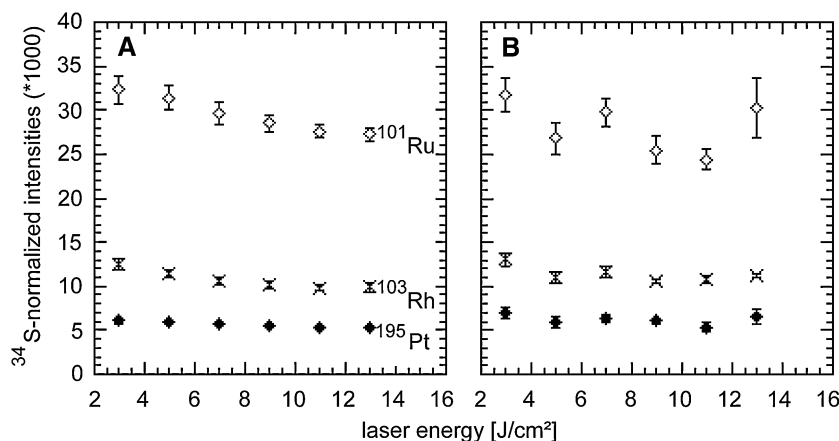


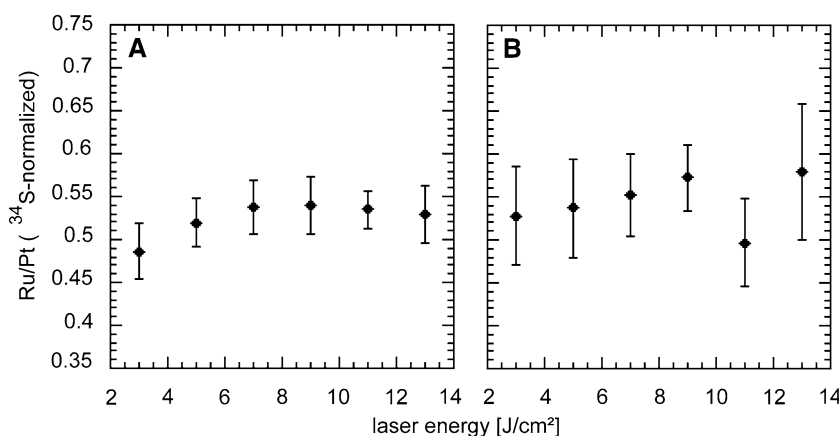
**Fig. 5** Effect of laser energy on the  $^{34}\text{S}$ -normalized count rates of the isotopes  $^{101}\text{Ru}$ ,  $^{103}\text{Rh}$ , and  $^{195}\text{Pt}$  (all  $\times 1000$ ), averages of 14 to 20 spectra from the  $(\text{Fe,Ni})_{1-x}\text{S}$  **a** and  $(\text{Fe,Cu})_{1-x}\text{S}$  **b** sulfide compositions. Error bars are 1 sigma variations



There is indeed energy-dependent isotopic fractionation. With increasing laser energy, all PGE/ $^{34}\text{S}$  count rate ratios decrease. Possibly, increasing the laser energy not only promotes sulfide melting (Fig. 4) but also selective sulfur degassing and perhaps sample oxidation, resulting in an energy dependent shift in the PGE/ $^{34}\text{S}$  ratios as observed in Fig. 5. In the more heterogeneous  $(\text{Fe,Cu})_{1-x}\text{S}$  composition, the trend is somewhat masked by compositional heterogeneities but none the less present. Fortunately though, the  $^{34}\text{S}$ -normalized count rate ratios, i.e.  $^{34}\text{S}$ -normalized count rates of noble metal isotopes divided by each other, are not strongly energy sensitive (Fig. 6). Hence, although target melting does occur in the sulfide target even at low to moderate laser energy, no significant relative noble metal isotopic fractionations can be resolved, and no element fractionation is noted according to monosulfide–sulfide melt Ds. Apparently, solid and liquid sulfide are ablated and ionized so efficiently and so rapidly that no significant PGE fractionation can occur.

The influence of the spot size on the relative errors is displayed in Fig. 7. The graph shows the averages of about 20 ablations with laser beam diameters of 25, 35, 60, and 120  $\mu\text{m}$ . Laser energy was kept constant at 5  $\text{J cm}^{-2}$ .

**Fig. 6** Effect of laser energy on the  $^{34}\text{S}$ -normalized count rate ratios of  $^{101}\text{Ru}/^{195}\text{Pt}$ , averages of 14 to 20 spectra from the  $(\text{Fe,Ni})_{1-x}\text{S}$  **a** and  $(\text{Fe,Cu})_{1-x}\text{S}$  **b** sulfide compositions. Error bars are 1 sigma variations

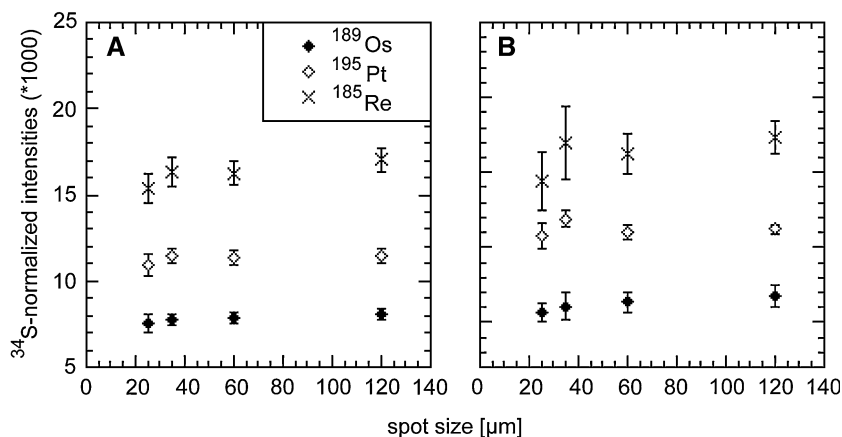


Representative for all isotopes, we present the  $^{34}\text{S}$ -normalized count rates of  $^{185}\text{Re}$ ,  $^{189}\text{Os}$ , and  $^{195}\text{Pt}$ , measured on the  $(\text{Fe,Ni})_{1-x}\text{S}$  and the  $(\text{Fe,Cu})_{1-x}\text{S}$  sulfide run products. Evidently, the effect of increasing the laser beam diameter is to enhance analytical precision, by increasing the ablation rate and integrating small-scale Re-PGE heterogeneities.

Analysis of standard compositions with isotope dilution-ICP-MS

Os, Ir, Ru, Pt, Pd and Re abundances were analysed by isotope dilution with an online analyte/matrix separation, using a quadrupole ICP mass spectrometer at the University of Leoben. Details of the analytical procedure are given by Meisel et al. (2003). The samples were digested in aqua regia in a high-pressure asher (HPA-S Anton Paar, Austria). Re, Os, Ir, Ru, Pt, and Pd were determined with isotope dilution, and element concentrations were calculated from isotopic ratios. Because Rh is monoisotopic, Rh concentrations had to be calculated from the other PGE count rates obtained during the on-line separation on the cation exchange column. Os concentrations were deter-

**Fig. 7** Influence of the laser beam diameter on the  $^{34}\text{S}$ -normalized count rates of the isotopes  $^{189}\text{Os}$ ,  $^{195}\text{Pt}$  and  $^{185}\text{Re}$  (\*1000), averages of 14 to 20 spectra from the  $(\text{Fe,Ni})_{1-x}\text{S}$  **a** and  $(\text{Fe,Cu})_{1-x}\text{S}$  **b** sulfide compositions. For laser beam diameters  $<60\ \mu\text{m}$  the 1 sigma variations tend to decrease with increasing spot size, implying that no heterogeneities exist on a scale larger than  $60\ \mu\text{m}$



mined by isotope ratio measurements following Hassler et al. (2000) and Meisel et al. (2001).

Results are given in Table 2. We note that the element concentrations added by micro syringe, i.e. 60 ppm Re and each PGE in the  $\text{Fe}_{1-x}\text{S}$  sulfide and 35 ppm in the  $(\text{Fe,Cu})_{1-x}\text{S}$  and  $(\text{Fe,Ni})_{1-x}\text{S}$  compositions, are reproduced rather well. This shows that during synthesis no significant element loss happens at any stage. Os and in part Pd tend to show greater variations among the aliquots analyzed, perhaps indicating some element-specific heterogeneities in the bulk sulfides. Note though that the RSD of the  $^{34}\text{S}$ -normalized laser count rates of  $^{189}\text{Os}$  and  $^{105}\text{Pd}$  are not systematically higher than those of the other noble metal isotopes. Rh proved to be problematic because Rh in solution appeared to be unstable and tended to precipitate with time. Therefore, only a few aliquots could be analyzed for Rh.

## Discussion

Sylvester et al. (2005) emphasized how important careful mechanical homogenization is to obtain chemically homogeneous sulfide standards. With this study, we show that the major element composition of the sulfide, the synthesis conditions, and the capsule material in which sulfide synthesis takes place are equally important parameters.

## Sulfide synthesis conditions

Sulfides are best synthesized from the elements. This permits the noble metals to be added as solutions, which is more precise than addition as metal powders or as other crystalline compounds. The solutions should be added to the elemental sulfur fraction before the major metals are added. If the acids come in contact with sulfide or the base metals from which sulfides are synthesized they will cause oxidation, adding oxygen to the charge and ultimately stabilizing in the run products undesired phases like magnetite.

The numerous mechanical homogenization steps recommended by Sylvester et al. (2005) do not guarantee homogeneous sulfides. Our sulfide compositions, with only one mechanical homogenization between 1-atm synthesis and sintering at high pressure, are at least as homogeneous. We recommend that the sulfide run products be sintered at high pressure before being used as laser standards. One-atm sulfides can be highly porous especially if they were synthesized at high  $\text{S}_2$  fugacity (low metal/S bulk ratio), whereas natural sulfides usually have theoretical densities. Sintering at high pressure ensures that both standard and unknown have similar densities. Differences in ablation behaviour due to matrix effects can thus be minimized.

**Table 2** Bulk noble metal contents of the  $\text{Fe}_{1-x}\text{S}$ ,  $(\text{Fe,Ni})_{1-x}\text{S}$ , and  $(\text{Fe,Cu})_{1-x}\text{S}$  sulfide compositions listed in Table 1. Rh analysed with solution ICP-MS, all other elements with isotope-dilution ICP-MS

Sulfide	Ru (ppm)	Rh (ppm)	Pd (ppm)	Re (ppm)	Os (ppm)	Ir (ppm)	Pt (ppm)
$\text{Fe}_{1-x}\text{S}$	$59.9 \pm 2.8$ (16)	$57.2 \pm 7$ (5)	$60.4 \pm 2.8$ (16)	$61.0 \pm 1.7$ (16)	$71.9 \pm 2.8$ (4)	$63.4 \pm 3.2$ (16)	$60.2 \pm 1.9$ (16)
$(\text{Fe,Ni})_{1-x}\text{S}$	$35.1 \pm 2.7$ (7)	34 (1)	$34 \pm 2$ (7)	$34.2 \pm 0.5$ (7)	36.9 (1)	$32.3 \pm 0.6$ (7)	$32.3 \pm 0.9$ (7)
$(\text{Fe,Cu})_{1-x}\text{S}$	$36.7 \pm 1.5$ (8)	$35.7 \pm 8.6$ (4)	$41.2 \pm 4.8$ (8)	$38.1 \pm 1.2$ (8)	$46.6 \pm 2.3$ (3)	$31.9 \pm 1.4$ (8)	$33.8 \pm 1.2$ (8)

(see text). Absolute uncertainties expressed as 1 sigma errors, number of determinations per element per sulfide composition given in brackets

### Influence of major elements on sample homogeneity

At least as important for homogeneity is the major element composition. For example, the concentration of vacancies on the metal sublattice of sulfide should be high because PGE substitution in sulfide is promoted by a high vacancy concentration (Ballhaus and Ulmer 1995; Li et al. 1996; Ballhaus et al. 2001). Therefore, sulfides to be used as standards should always be synthesized with a slight (5–10 mol%) sulfur excess in the starting mix. The cation spectrum also plays a role. Our most homogeneous compositions are the pure  $\text{Fe}_{1-x}\text{S}$  and the Ni-bearing  $\text{Fe}_{1-x}\text{S}$  monosulfides. Cu in  $(\text{Fe,Cu})_{1-x}\text{S}$ , in contrast, appears to promote noble metal heterogeneity, possibly because Cu itself is not so well soluble in FeS-dominated monosulfide solid solutions as Ni (Ballhaus et al. 2001). In nature, the Cu content is one of the factors driving exsolution and recrystallization of high-temperature multi-component  $(\text{Fe,Ni,Cu})_{1-x}\text{S}$  monosulfide, and this could also impose PGE heterogeneity. We could not verify exsolution structures in our  $(\text{Fe,Cu})_{1-x}\text{S}$  composition, however, in view of the modest quenching rates achieved with piston-cylinder presses (about 20 s to  $<100^\circ\text{C}$ ) and the enormous reactivity of sulfide upon cooling (Ballhaus and Ulmer 1995; Etschmann et al. 2004) exsolutions on a sub-micron scale are likely to be there.

NiS seems to be an unsuitable matrix for a PGE sulfide standard. Ni–S sulfides do not seem to have the flexibility in terms of metal/S ratios as Fe-dominated monosulfides. Therefore, if the bulk metal/S ratio does not match exactly the stoichiometry of a particular Ni sulfide, several phases with different metal/S atomic ratios will crystallize, potentially causing noble metal to fractionate between the phases. FeS-based bulk compositions, in contrast, will usually crystallize only one  $\text{Fe}_{1-x}\text{S}$  phase with flexible metal/S stoichiometry, so long as atomic metal/S is between 1 and about 0.88. We consider this to be an important result and recommend not to use NiS fire assay buttons as laser sulfide standards.

The form in which noble metal heterogeneities occur, whether as patchy distributions in solid solution or as discrete PGE sulfides or alloys, is uncertain. Laser ablation spectra of heterogeneous sulfides frequently display discrete PGE peaks, and therefore, we tend to favour discrete PGE phases. Note though that no discrete PGE phases were identified in BSE images even in the most heterogeneous sulfide compositions, despite careful search.

### Influence of capsule material on sample homogeneity

Whenever a charge was sintered in boron nitride or graphite capsules, we noted much enhanced noble metal heterogeneity compared to sulfides sintered in  $\text{SiO}_2$ . Evi-

dently, there is a reaction between these substances and sulfide at run conditions, and this reaction lowers Re-PGE solubility. Major elements and the metal/S atomic ratios are unaffected. The only reasonable reaction we can imagine is reaction with oxygen, since both BN and graphite are highly reducing compounds and would tend to extract any oxygen present in the sulfide. However, if this is correct it would imply that crystalline sulfides contain significant quantities of oxygen in the lattices. More importantly, it would mean that oxygen in solid solution in sulfide may be a factor that influences the solubility of noble metals in base metal sulfides.

### Melting under the laser beam

Partial sulfide melting seems unavoidable even at low laser energies, despite the short wavelength of the excimer laser. For noble metal analysis, melting is not necessarily a problem. We do observe systematic shifts in  $^{34}\text{S}$ -normalized noble metal count rates with increasing laser beam energy (Fig. 5) which may be related to melting and selective sulfur outgassing, but this effect disappears if we divide  $^{34}\text{S}$ -normalized noble metal count rates by each other (Fig. 6). The implication is that crystalline sulfide and sulfide melt are ablated to about the same extent. Nonetheless, every effort should be made to minimize sample melting. Whenever crystalline sulfide coexists with sulfide melt, there is the danger that chalcophile elements with very large or very small monosulfide–sulfide melt partition coefficients ( $D$ ) may fractionate between the phases, resulting in systematic PGE heterogeneities that will depend on both the laser energy and the magnitude in the  $D$ s. It is advised, therefore, that standards and sulfide unknowns have similar compositions and are analyzed with the same laser energies and laser frequencies, so that element fractionations by partial melting may cancel each other.

### Conclusions

1. Synthesis of noble metal standards in sulfide matrix for destructive laser-ablation ICP-MS analysis is not difficult if a few principles are observed. In addition to careful mechanical homogenization, other factors important for standard homogeneity are the major element matrix and the synthesis conditions. Sintering at high pressure is important to ensure that standards and sulfide unknowns both have theoretical densities.
2. Controlled sulfide synthesis, preferably from metals and elemental sulfur, is superior to standard production by segregating NiS sulfide melt from a HSE-bearing

silicate melt (NiS fire assay). The noble metal abundances in sulfide, especially if they are added as solutions via microsyringe, can be controlled more precisely than by fire assay collection. Fe-dominated monosulfides are more flexible with respect to atomic metal/S stoichiometry than Ni-rich monosulfides. Therefore, FeS-dominated sulfide charges can be quenched to a single crystalline  $\text{Fe}_{1-x}\text{S}$  phase over a much wider metal/S range than NiS-dominated sulfide compositions. Noble metal heterogeneities by small-scale quench redistribution between phases with variable metal/S stoichiometries can thus be avoided.

- Our synthetic  $\text{Fe}_{1-x}\text{S}$  and  $(\text{Fe,Ni})_{1-x}\text{S}$  monosulfide compositions are among the most homogeneous noble metal sulfides synthesized to date. Moreover, they are the only standards reported in the literature that contain Re in addition to the PGE.
- The sulfides will be used as noble metal standards for LA-ICPMS analysis. Aliquots can be made available upon request.

**Acknowledgements** Financial support by the DFG to Chris Ballhaus (grant Ba 964/24-1) is gratefully acknowledged. The final manuscript has benefited from a thorough and insightful review by Paul Sylvester and an anonymous reviewer.

## References

- Alard O, Griffin WL, Lorand JP, Jackson SE, O'Reilly SY (2000) Non-chondritic distribution of the highly siderophile elements in mantle sulphides. *Nature* 407:891–894
- Ballhaus C, Stumpfl EF (1986) Sulfide and platinum mineralization in the Merensky reef: evidence from hydrous silicates and fluid inclusions. *Contrib Miner Petrol* 94:193–204
- Ballhaus C, Ryan CG (1995) Platinum-group elements in the Merensky reef. I. PGE in solid solution in base metal sulfides and the down-temperature equilibration history of Merensky ores. *Contrib Miner Petrol* 122:241–251
- Ballhaus C, Ulmer P (1995) Platinum-group elements in the Merensky reef. 2. Experimental solubilities of platinum and palladium in Fe1-Xs from 950 to 450°C under controlled fS2 and fH2. *Geochim Cosmochim Acta* 59:4881–4888
- Ballhaus C, Sylvester P (2000) Noble metal enrichment processes in the Merensky reef, Bushveld complex. *J Petrol* 41:545–561
- Ballhaus C, Tredoux M, Spaeth A (2001) Phase relations in the Fe–Ni–Cu–PGE–S system at magmatic temperature and application to massive sulfide ores of the Sudbury igneous complex. *J Petrol* 42:1911–1926
- Ballhaus C, Bockrath C, Wohlgemuth-Ueberwasser C, Laurenz V, Berndt J (2006) Fractionation of the noble metals by physical processes. *Contrib Mineral Petrol* 152:667–684
- Barnes SJ, Cox RA, Zientek ML (2006) Platinum-group element, gold, silver and base metal distribution in compositionally zoned sulfide droplets from the Medvezky creek mine, Noril'sk, Russia. *Contrib Mineral Petrol* 152:187–200
- Bockrath C, Ballhaus C, Holzheid A (2004a) Fractionation of the platinum-group elements during mantle melting. *Science* 305:1951–1953
- Bockrath C, Ballhaus C, Holzheid A (2004b) Stabilities of laurite RuS2 and monosulfide liquid solution at magmatic temperatures. *Chem Geol* 208:265–271
- Cabri LJ, Sylvester PJ, Tubrett MN, Peregoedova A, Laflamme LHG (2003) Comparison of LAM-ICP-MS and Micro-PIXE results for palladium and rhodium in selected samples of Noril'sk and Talnakh sulfides. *Can Mineral* 41:321–329
- Chenery S, Cook JM, Styles M, Cameron EM (1995) Determination of the three-dimensional distributions of precious metals in sulphide minerals by laser ablation microprobe-inductively coupled plasma-mass spectrometry (LAMP-ICP-MS). *Chem Geol* 124:55–65
- Date AR, Davis AE, Cheung YY (1987) The potential of fire assay and inductively coupled plasma mass spectrometry for the determination of platinum group elements in geological materials. *Analyst* 112:1217–1222
- Eggins SM, Kinsley LPJ, Shelley JMG (1998) Deposition and element fractionation processes during atmosphere pressure laser sampling for analysis by ICP-MS. *Appl Surf Sci* 127–129:278–286
- Etschmann B, Pring A, Putnis A, Grguric BA, Studer A (2004) A kinetic study of the exsolution of pentlandite  $(\text{Ni,Fe})_9\text{S}_8$  from the monosulfide solid solution  $(\text{Fe,Ni})\text{S}$ . *Am Mineral* 89:39–50
- Gervilla F, Kojonen K (2002) The platinum-group minerals in the upper section of the Keivitsansarvi Ni–Cu–PGE deposit, northern Finland. *Can Mineral* 40:377–394
- Günther D, Heinrich CA (1999) Enhanced sensitivity in laser ablation-ICP mass spectrometry using helium–argon mixtures as aerosol carrier—Plenary lecture. *J Anal At Spectr* 14:1363–1368
- Hassler DR, Peucker-Ehrenbrinck B, Ravizza GE (2000) Rapid determination of Os isotopic composition by sparging OsO4 into a magnetic-sector ICP-MS. *Chem Geol* 166:1–14
- Helmy HM, Ballhaus C, Berndt J, Bockrath C, Wohlgemuth-Ueberwasser C (2007) Formation of Pt, Pd and Ni tellurides: experiments in sulfide-telluride systems. *Contrib Mineral Petrol* 153:493–624
- Horn I, Guillong M, Günther D (2001) Wavelength dependent ablation rates for metals and silicate glasses using homogenized laser beam profiles—implications for LA-ICP-MS. *Appl Surf Sci* 183:91–102
- Huminić MAE, Sylvester PJ, Cabri LJ, Leshner CM, Tubrett M (2005) Quantitative mass balance of platinum group elements in the Kelly Lake Ni–Cu–PGE deposit Copper Cliff offset, Sudbury. *Econ Geol* 100:1631–1646
- Jackson SE, Fryer BJ, Gosse W, Healey DC, Longerich HP, Strong DF (1990) Determination of precious metals in geological materials by inductively coupled plasma-mass spectrometry (ICP-MS) with nickel sulphide fire-assay collection and tellurium coprecipitation. In: Potts PJ, Dupuy C and Bowles JFW (Eds), *Microanalytical methods in mineralogy and geochemistry*. *Chem Geol* 83:119–132
- Jarvis KE, Williams JG, Parry SJ, Bertalan E (1995) Quantitative determination of the platinum-group elements and gold using NiS fire assay with laser ablation-inductively coupled plasma-mass spectrometry (LA-ICP-MS). *Chem Geol* 124:37–46
- Jorge AP de S, Enzweiler J, Shibuya E, Sarkis JES, Figueiredo AMG (1998) Platinum-group elements and gold determination in NiS fire assay buttons by UV laser ablation ICP-MS. *Geostand News* 22:47–55
- Lehner SW, Savage KS, Ayers JC (2006) Vapor growth and characterization of pyrite (FeS2) doped with Co, Ni, and As: variations in semiconducting properties. *J Cryst Growth* 286:306–317
- Li C, Barnes SJ, Makovicky E, Rose-Hansen J, Makovicky M (1996) Partitioning of nickel, copper, iridium, rhenium, platinum, and palladium between monosulfide solid solution and sulfide liquid:

- effects of composition and temperature. *Geochim Cosmochim Acta* 60:1231–1238
- McDonald I (2005) Development of sulphide standards for the in-situ analysis of platinum-group elements by laser ablation inductively coupled plasma-mass spectrometry (LA-ICP-MS). Abstract, 10th Intern Platinum Symp:468–471
- Meisel T, Moser J, Fellner N, Wegscheider W, Schoenberg R (2001) Simplified method for the determination of Ru, Pd, Re, Os, Ir and Pt in chromitites and other geological materials by isotope dilution ICP-MS and acid digestion. *Analyst* 126:322–328
- Meisel T, Fellner N, Moser J (2003) A simple procedure for the determination of platinum group elements and rhenium (Ru, Rh, Pd, Re, Os, Ir and Pt) using ID-ICP-MS with an inexpensive on-line matrix separation in geological and environmental materials. *J Anal At Spectr* 18:720–726
- Miller JD, Li J, Davidtz JC, Vos F (2005) A review of pyrrhotite flotation chemistry in the processing of PGM ores. *Miner Eng* 18:855–865
- Mungall JE, Andrews DRA, Cabri LJ, Sylvester PJ, Tubrett M (2005) Partitioning of Cu, Ni, Au, and platinum-group elements between monosulfide solid solution and sulfide melt under controlled oxygen and sulfur fugacities. *Geochim Cosmochim Acta* 69:4349–4360
- Perkins WT, Pearce NJG, Westgate JA (1997) The development of laser ablation ICP-MS and calibration strategies: Examples from the analysis of trace elements in volcanic glass shards and sulfide minerals. *Geostand Newsl* 21:175–190
- Shibuya EK, Sarkis JES, Enzweiler J, Jorge APS, Figueiredo AMG (1998) Determination of platinum group elements and gold in geological materials using an ultraviolet laser ablation high-resolution inductively coupled plasma mass spectrometry technique. *J Anal At Spectr* 13:941–944
- Sylvester PJ, Cabri LJ, Tubrett MN, McMahon, G, Laflamme JHG, Peregoedova A (2005) Synthesis and evaluation of a fused pyrrhotite standard reference material for platinum group element and gold analysis by laser ablation-ICPMS. Abstract, 10th Intern Platinum Symp, 16–20
- Wilson SA, Ridley WI, Koenig AE (2002) Development of sulfide calibration standards for the laser ablation inductively-coupled plasma mass spectrometry technique. *J Anal At Spectr* 17:406–409
- Yang XM, Lentz DR, Sylvester PJ (2006) Gold contents of sulfide minerals in granitoids from southwestern New Brunswick, Canada. *Miner Dep* 41:369–386